Aerosol Res., 2, 225–233, 2024
https://doi.org/10.5194/ar-2-225-2024

AEROSOL Research
Open Access

Direct detection of polycyclic aromatic hydrocarbons on a molecular composition level in summertime ambient aerosol via proton transfer reaction mass spectrometry

Tobias Reinecke, Markus Leiminger, Andreas Klinger, and Markus Müller

IONICON Analytik GmbH, 6020 Innsbruck, Austria

Correspondence: Markus Müller (markus.mueller@ionicon.com)

Received: 28 March 2024 – Discussion started: 16 April 2024
Revised: 26 June 2024 – Accepted: 4 July 2024 – Published: 18 July 2024

Abstract. Condensed particulate polycyclic aromatic hydrocarbons (PAHs) are a group of toxic organic compounds that are produced by the incomplete combustion of organic material, for example, via biomass burning or traffic emissions. Even at low long-term exposure levels, such as 1 ng m^{-3} of benzo(a)pyrene, PAHs are recognized to be detrimental to human health. Therefore, a quantitative characterization of PAHs at sub-nanogram-per-cubic-meter levels is important to examine precise long-term exposure.

A new ultrasensitive generation of proton transfer reaction mass spectrometry (PTR-MS) instruments coupled to the CHARON particle inlet are capable of quantitatively detecting this toxic class of compounds at a molecular composition level while also offering a high temporal resolution of < 1 min and sub-nanogram-per-cubic-meter limits of detection. To demonstrate the capabilities of this new CHARON FUSION PTR-TOF 10k instrument, we present a thorough characterization of summertime ambient condensed PAHs in Innsbruck, Austria. With a mass resolution of $> 14\,000$ (m Δm^{-1} at full width at half maximum) and sensitivities of up to 40 cps ng^{-1} m^3 (where cps represents counts per second), a series of nine condensed PAHs of four ($C_{16}H_{10}$) to six aromatic rings ($C_{26}H_{16}$) are identified among a plethora of organic compounds in ambient organic aerosol. With 1 min limits of detection between 19 and 46 pg m^{-3}, quantitative time series of these PAHs at the lowermost mass concentrations are determined.

To understand the sources and processes associated with these condensed summertime PAHs in greater detail, a matrix factorization including the $\sim$4000 ionic signals detected by the CHARON FUSION PTR-TOF 10k is performed, representing the vast majority of the mass concentration of ambient organic aerosol. A total of 10 factors and their corresponding time series can be identified. Known tracer compounds like levoglucosan, pinonic acid or nicotine consequently allow the assignment to individual organic aerosol sources and physicochemical processes. PAH emissions from traffic are found to be minor contributors during this summertime sampling period. The highest concentrations of PAHs are identified in a mixed aged oxygenated organic aerosol, followed by a biomass burning and a cigarette smoke organic aerosol.

1 Introduction

Polycyclic aromatic hydrocarbons (PAHs) are a group of toxic organic compounds that are formed through the incomplete combustion of organic materials. Common sources are biomass burning, industrial processes, transportation and waste incineration (Kaur et al., 2013). PAHs are recognized as causing mutagenic, carcinogenic, teratogenic and immunotoxicogenic effects (Agudelo-Castañeda et al., 2017). Even at low long-term exposure levels, such as 1 ng m^{-3} of the commonly found benzo(a)pyrene, PAHs can be detrimental to human health (Choi et al., 2010). Once released, the semi-volatile nature of many PAHs, i.e., typically PAHs with more than three to four aromatic rings, leads to condensation onto ambient particles. Consequently, these particles are

known to be widely spread via long-range transport prior to deposition on soil, plants and water.

Although they belong to a toxic compound class that is released by various sources, the detection of PAHs can be challenging due to the semi-volatile nature and chemical properties of the most abundant PAHs. High-throughput filter-based methods followed by desorption of the PAHs and analysis via high-performance liquid chromatography (HPLC) or gas chromatography (GC) have proven to be very sensitive methods with low limits of detection (Thrane and Mikalsen, 1981; Borrás and Tortajada-Genaro, 2007; Lung and Liu, 2015). However, these methods are prone to sampling artifacts, for example, due to the evaporation of the more volatile PAHs during sampling (Patel et al., 2020). Moreover, sample handling, storage and analysis are elaborate and consume substantial resources. Additionally, filter measurements suffer from low temporal resolution; therefore, source apportionment based on these data might miss important factors caused by diurnal or even shorter-term features.

In recent years, several direct methods based on mass spectrometry have been developed (Laskin et al., 2018). The aerosol mass spectrometer (AMS; Aerodyne Research Inc., USA) is probably the most commonly used instrument, allowing the characterization of total submicrometer particulate PAHs within single minutes and single-digit nanogram-per-cubic-meter mass concentrations (Dzepina et al., 2007; Poulain et al., 2011; Eriksson et al., 2014; Herring et al., 2015; Xu et al., 2022). However, due to interference and fragmentation caused by electron ionization on a 600 °C hot surface, the AMS is not able to provide data on individual PAH species. Other mass spectrometric techniques are based on laser desorption or ionization for a single-particle-based analysis. One instrument featuring a highly selective and soft laser ionization of PAHs is the resonance-enhanced multiphoton ionization (REMPI) time-of-flight (TOF) spectrometer (Schade et al., 2019; Passig et al., 2022). The REMPI-TOF provides valuable insights, including single-particle PAH distributions in aerosols, and additionally allows for an assignment of the detected particles to specific pollution sources. However, single-particle instruments do not provide mass concentrations of PAHs.

In contrast to these either hard or highly selective ionization techniques, soft chemical ionization mass spectrometry (CIMS) can conserve chemical information and only exhibits a small amount of ionization-induced fragmentation. While certain CIMS instruments might be sensitive to derivatives of PAHs, with, for example, nitro or oxygenated functional groups that are often referred to as polycyclic aromatic compounds (PACs), most of these instruments cannot or can hardly directly detect and quantify PAHs, as the chemical properties of PAHs, especially the low proton affinity, prevent efficient ionization. One exception – CIMS that is highly capable of detecting PAHs – is proton transfer reaction mass spectrometry (PTR-MS).

PTR-MS is a soft chemical ionization technique that can quantitatively detect a plethora of volatile organic compounds (VOCs) in real time (Hansel et al., 1995; Graus et al., 2010; Yuan et al., 2017). It utilizes ion–molecule reactions of VOCs with H_3O^+ primary reagent ions in a well-controlled reaction environment. PTR-MS has already proven to be able to detect and quantify PAHs on a molecular composition level without ionization-induced fragmentation (e.g., Gueneron et al., 2015). With the CHARON particle inlet for PTR-MS (Eichler et al., 2015), this capability is extended to PAHs that are condensed onto particles (Müller et al., 2017; Piel et al., 2019). Side-by-side measurements of CHARON PTR-TOF and high-throughput filter samples at the research station in Melpitz, Germany, operated by the Leibniz Institute for Tropospheric Research (TROPOS; Leipzig, Germany), have already resulted in good qualitative and quantitative agreement on a 24 h basis (Wisthaler et al., 2020). However, the CHARON PTR-TOF instrument was able to provide significantly higher temporal resolution, even at single-digit nanogram-per-cubic-meter mass concentrations.

For this study, we have modified a new ultrasensitive PTR-MS instrument, the so-called FUSION PTR-TOF 10k (Reinecke et al., 2023), to be successfully paired to a further improved version of CHARON. To demonstrate the capabilities of this instrument to detect ultralow mass concentrations of a series of PAHs, a dataset was acquired in summertime in Innsbruck, Austria, during 11 consecutive days. Based on this dataset, we show that the CHARON FUSION PTR-TOF 10k achieves detection limits down to low double-digit picogram-per-cubic-meter mass concentrations for PAHs. To further understand the sources and processes associated with these PAHs, we apply matrix factorization to the entire recorded dataset of $\sim$4000 recorded ions, representing the vast majority of the mass concentrations of organic compounds in ambient aerosol.

2 Methods

2.1 FUSION PTR-TOF 10k

The FUSION PTR-TOF 10k was recently introduced by Reinecke et al. (2023). In a nutshell, the FUSION PTR-TOF 10k is an ultrahigh-sensitivity PTR-MS instrument that reaches sensitivities of up to 80 cps pptv^{-1} (where cps represents counts per second and pptv represents parts-per-trillion volume mixing ratio) and limit of detection (LOD) values in a sub-parts-per-trillion volume ratio range while simultaneously conserving the well-defined ion chemistry of conventional PTR-MS.

With the novel fast-selective reagent ion (SRI) ion source (see Reinecke et al., 2023, for details), H_3O^+ primary reagent ions are generated in a H_2O plasma discharge at the highest purity, while neutral interferences like the hydroxyl radical (OH) are significantly reduced. These H_3O^+ primary reagent ions subsequently react with the VOCs of a sam-

ple gas inside the newly developed FUSION ion–molecule reactor to produce protonated VOCs ($VOC.H^+$). Here, a stack of concentric ring electrodes generates a static longitudinal electric field superimposed by a focusing transversal radio frequency (RF) field, maximizing the ion transfer into the TOF-MS. The well-controlled ion–molecule reaction conditions enable a quantitative ionization of a wide range of VOCs, from nonpolar compound classes like aromatic species and PAHs to highly polar ones like highly oxidized organic molecules (HOMs). Finally, the ions are detected by TOF-MS with a mass resolution ($m\,\Delta m^{-1}$ at full width at half maximum; FWHM) in a range of 10 000 to 15 000. This mass resolution is sufficiently high to directly assign chemical compositions to the detected exact m/z.

Herein, the FUSION PTR-TOF 10k was operated at a reaction chamber temperature of 120 °C and a moderate reduced electric field strength of $E/N = 100$ Td ($1\,\text{Td} = 10^{-17}\,\text{V cm}^2$; with E being the electrical field strength in the ion–molecule reactor and N being the number density of the sample gas the ion–molecule reactor). Together with the extended volatility range (EVR) coating of both the inlet and the FUSION RF ion–molecule reactor, low-volatility organic compounds can be detected with quick instrumental response times (Piel et al., 2021).

The original design of the FUSION PTR-TOF 10k reported by Reinecke et al. (2023) used an inlet flow of 100–120 mL min^{-1}. This flow is significantly higher than in standard PTR-MS (i.e., in the range of 15–25 mL min^{-1}) and exceeds the capability of the aerodynamic lens system of the CHARON particle inlet. Therefore, the FUSION RF ion–molecule reactor and inlet system were redesigned to accommodate a lower inlet flow rate in the range of 20 mL min^{-1} and, thus, ensure compatibility with the CHARON particle inlet.

2.2 CHARON particle inlet

With the Chemical Analysis of oRganic particles ON-line (CHARON) particle inlet, the capability of a PTR-TOF instrument to measure volatile organics is extended to the particle phase (Eichler et al., 2015; Müller et al., 2017). The CHARON consists of a charcoal monolith denuder to remove the gas phase with an efficiency of > 99.999 % for, for example, acetone. Simultaneously, more than 90 % of the particles above 70 nm are transmitted through the charcoal monolith denuder. These particles are then collimated by a high-pressure aerodynamic lens system operated at 7.5 mbar and a flow of ∼ 450 mL min^{-1}. An enriched particle stream (∼ 20 mL min^{-1}) is subsampled by means of a virtual impactor, while the majority of residual gas is pumped away. Under the assumption that the particles are being subsampled, this setup allows for a theoretical particle enrichment by a factor 22.5. Finally, the volatile fraction of the particles is efficiently evaporated in a thermal desorption unit at reduced pressures (< 7.5 mbar) and moderate temperatures of 160 °C. All volatilized organics are consequently detected in the gas phase with a PTR-TOF instrument. Zero calibration of the CHARON is achieved by redirecting the aerosol sample flow through a high-efficiency particulate absorbing (HEPA) filter.

For this study, an aerodynamic lens system geometry that was optimized by computational fluid dynamics (CFD) was tested; this geometry successfully increased the detectable particle size range by roughly 20 nm towards smaller particle sizes compared with earlier versions of CHARON. The range of near-constant particle transmission (herein defined as ±20 %) now covers ∼ 100 nm up to > 1 µm (instead of ∼ 120 nm up to > 1 µm). Particles in a size range from 60 to 100 nm are still detected, but they are observed with a reduced particle enrichment efficiency (see Fig. S1 in the Supplement for the measured particle enrichment efficiency as a function of the particle size).

With this setup, organics with a saturation mass concentration of $\log C^0_{300\,\text{K}} > -5$, which includes parts of extremely low volatility organic compounds (ELVOCs) as well as the full range of low-volatility and semi-volatile organic compounds (LVOCs and SVOCs, respectively), can be completely evaporated and detected in real time. Figure S2 demonstrates this real-time response of the CHARON FUSION PTR-TOF 10k for polydisperse levoglucosan particles (SVOCs, $\log C^0_{300\,\text{K}} \sim 0$) with a mass concentration of roughly 0.5 µg m^{-3}. After switching to HEPA, a $1/Eu$ decay (i.e., a decay to 36.8 % of the initial signal) is reached within 8 s and a decay down to 10 % within 31 s.

2.3 Site description and meteorological conditions

The CHARON FUSION PTR-TOF 10k was deployed in Innsbruck, Austria, from 18 to 28 August 2023. The measurements were conducted at the IONICON Analytik laboratory, located in the east of Innsbruck. The aerosol was sampled from the outside through a 1/4 in., stainless-steel, < 2 m (total length) tube with a flow rate of 0.5 L min^{-1}. A planned power line service on the afternoon of 24 August caused an overnight data acquisition interruption.

The sampling period mostly fell within a stable high-pressure period with low wind and elevated temperatures (ranging from 17 to 34 °C). A clear change in the weather pattern to high winds and lower temperatures was observed towards the end of the period. Figure 1a displays the ambient temperature and the ozone mass concentration as measured at a close-by air quality site, Innsbruck Reichenau – Andechsstraße, operated by the Austrian Umweltbundesamt (Environment Agency Austria; https://luft.umweltbundesamt.at/pub/gmap/start.html#, last access: 11 July 2024).

The general meteorological conditions in Innsbruck, which is an urban, alpine environment, are described in detail by Karl et al. (2020). In brief, Innsbruck is a major city located in the Inn River valley at 570 m above sea level; the

valley is oriented from west to east and is surrounded by mountains with elevations of up to 2500 m in the north and south that constrain air mass exchange. Local emissions from a typical mixture of urban, industrial and nearby agricultural sources are complemented by biogenic emissions from forests, which cover the mountain slopes, and transit traffic emissions, as the Inn River valley acts as the major transit route connecting Germany and Italy.

2.4 Data acquisition

All data were recorded with a 10 s time resolution, and mass spectra ranged up to m/z 719. To increase the separation capability of isobaric ions, an enhanced upper-limit mass-resolution of the TOF-MS of $> 14\,000$ (FWHM) was selected (instead of the rated mass resolution of 10 000). We automatically conducted frequent zeros every 6 h by switching to CHARON HEPA mode to remove the particle phase from the ambient air sample. A calibration with a dynamically diluted VOC standard was conducted prior to the measurement period to determine the transmission function of the instrument. The validity of this transmission function was checked at the end of the measurement period and was found to agree within a deviation of 10 %. Sensitivities of the FUSION PTR-TOF 10k operated at mass resolutions of 14 000 were in the range of 15 to 20 cps pptv^{-1} for most VOCs in the calibration gas standard. With the CHARON particle inlet, this roughly corresponds to a sensitivity of ~ 40 cps ng^{-1} m^3 for particulate PAHs.

2.5 Data analysis

Data analysis was performed with the IONICON Data Analyzer (IDA), version 2.2.0.4 (Müller et al., 2013). The IDA provides project management, high temporally and m/z-resolved peak analysis, and quantification of PTR-TOF datasets with high precision and accuracy. The IDA's high level of automation and parallelization allows for fast analysis results for complex datasets like the CHARON particle spectra, which often include thousands of ionic signals.

To enable quantification of the dataset, the instrumental transmission function is combined with reaction rate constants (k rate). The reaction rate constants of the compounds are calculated from the polarizability, obtained from a parameterization based on the respective chemical composition (Bosque and Sales, 2002), and the dipole moment, based on the parameterization proposed by Sekimoto et al. (2017), by applying the Su–Chesnavich parameterization of ion–polar molecule collisions (Su and Chesnavich, 1982). We estimate the combined accuracy of the transmission function and the parameterized k rates in the range of ± 30 %. CHARON bulk information was corrected for fragmentation, as introduced by Leglise et al. (2019). With this fragmentation correction, CHARON is typically able to quantify between 80 % and 100 % of the total organic aerosol.

In a first analysis step, monoaromatic and polyaromatic compounds are tentatively identified via the aromaticity equivalent X_C (Yassine et al., 2014). With the number (no.) of C, N, H and O atoms and with m as the fraction of the oxygen atoms involved in the π-bond structure for a given organic compound, X_C is calculated according to Eq. (1):

$$X_C = \frac{2\,\text{no. C} + \text{no. N} + \text{no. H} - 2\text{m no. O}}{\text{RDBE} - \text{m no. O}} + 1$$
$$\text{with RDBE} = 1 + \frac{1}{2}(2\,\text{no. C} - \text{no. H} + \text{no. N}). \quad (1)$$

Subsequently, pure hydrocarbons C_xH_y with a ring and double-bond equivalent (RDBE) ≥ 7 and with $x > y$ are identified as PAHs (with x being the number of C atoms and y the number of H atoms), as introduced for CHARON PTR-TOF by Piel et al. (2019).

To better understand the sources and processes associated with the detected signals, a nonnegative matrix factorization (NMF) was performed. This NMF is initialized via a nonnegative double singular-value decomposition (NNDSVD), as described by Boutsidis and Gallopoulos (2008). This NNDSVD initialization approach leads to a rapid reduction in the approximation error of NMF and is, therefore, well suited for the factorization of large datasets like the one presented herein, which includes thousands of time series of ionic signals with each consisting of more than 100 000 data points. In addition, similar to positive matrix factorization (PMF), which is frequently used in aerosol research (e.g., Ulbrich et al., 2009), this method results in a quantitative and qualitative reconstruction of time series and mass spectral information. The optimal number of factors is selected via a cost function and a cross-correlation matrix of the corresponding time series and mass spectra.

3 Results and discussion

3.1 Identification and quantification of PAHs

Figure 1 depicts the time series of the ambient temperature and the ozone mass concentration, as published by the Austrian Umweltbundesamt, as well as the total signal of condensed organics and the average mass spectrum, as recorded by CHARON FUSION PTR-TOF 10k, during the measurement period from 18 to 28 August 2023. Again, we note that the measurement was unfortunately interrupted at around noon on 24 August; hence, there is an 18 h gap in the recorded data.

Initially, in the period from 18 to 25 August, the total organic mass concentration slowly ramps up from a daily maximum below 1.5 µg m^{-3} to almost 5 µg m^{-3}, with highest mass concentrations in the noon hours. The visually clear correlation with ozone mass concentrations indicates the significance of secondary particle formation processes during this period. Starting in the early morning of 27 August,

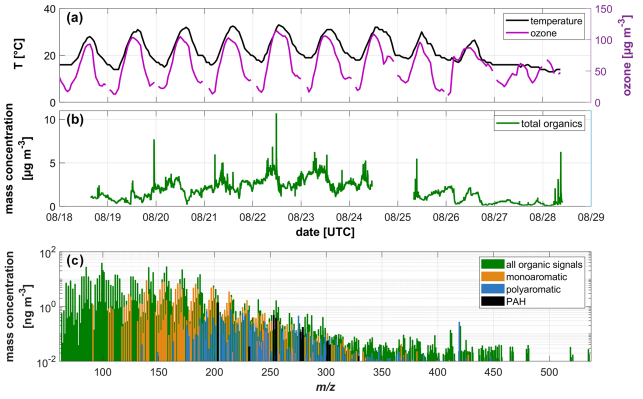

Figure 1. Ambient temperature and ozone concentrations, published by the Austrian Umweltbundesamt **(a)**; the mass concentration of total organics **(b)**; and the instrumental background-corrected average mass spectrum **(c)**, as recorded by the FUSION PTR-TOF 10k. Color codes of the average mass spectrum reflect all detected organic signals (green), compounds that are tentatively identified as monoaromatics (orange; $2.5 \leq X_C < 2.71$, $m = 0$) or polyaromatics (blue; $X_C \geq 2.71$, $m = 0$), and the assigned PAHs (black; RDBE ≥ 7).

the initial stable high-pressure system gets replaced by considerably colder, stormy and wet conditions. As expected, with this weather change, the particle concentration is significantly decreased, with average mass concentrations below 1 µg m^{-3}. Despite this general trend, frequent short-term spikes, especially during working days (i.e., 21–26 and 28 August), show the presence of local particle emission sources with mass concentrations of up to 11 µg m^{-3}.

The average mass spectrum (Fig. 1c) underlines the chemical complexity of the vaporized condensed organics. Repetitive groups of chemical compositions up to m/z 350 are visible, representing compounds of various oxidation states. To further understand the chemical composition of the detected ionic signals, we have calculated the aromaticity equivalent X_C to visualize an upper limit ($m = 0$) of monoaromatic ($2.5 \leq X_C < 2.71$) and polyaromatic ($X_C \geq 2.71$) signals. Black bars highlight the detected PAHs that are C_xH_y signals of RDBE ≥ 7 with $x > y$. In total, nine PAH-related ionic signals are identified that range from $C_{16}H_{11}^+$ (m/z 203.086; four-ring PAHs, e.g., pyrene, fluoranthene and other isomers) to $C_{26}H_{17}^+$ (m/z 329.133; six-ring PAHs, e.g., hexacene). With the exception of $C_{16}H_{11}^+$, all PAH signals show an average mass concentration of well below 1 ng m^{-3}.

Figure 2a, b and c depict three peak systems that include the PAH signals $C_{20}H_{13}^+$, $C_{20}H_{15}^+$ and $C_{22}H_{15}^+$, respectively. The complexity of these peak systems illustrates the importance of an instrument with a high mass resolution to distinguish the PAH signals from the multitude of surrounding peaks. However, even at m Δm$^{-1} > 14\,000$ (FWHM), peak separation remains challenging. Nonetheless, a total of nine ionic signals from PAHs detected in the particle phase (from $C_{16}H_{11}^+$ to $C_{26}H_{17}^+$) were extracted from our dataset. The time series of these PAHs are plotted in Fig. 2d and e. The highest average mass concentrations are visible for $C_{16}H_{11}^+$ (e.g., pyrene and isomers), whereas most spikes are dominated by $C_{18}H_{15}^+$, i.e., the sum of benzofluoranthenes and benzopyrenes. Figure 2e shows a close-up of the late hours of 19 August, where the largest of all PAH spikes was recorded. This is a good example to assess the instrumental response time to our compounds of interest in the experimental environment: all PAHs react quickly to this concentration increase and also drop quickly to previous background concentrations once the recorded plume has passed. In addition, this figure also indicates the extremely low noise levels of the recorded data. Even during this local emission event, most PAHs do not exceed 1 ng m^{-3} levels. Based on the frequent HEPA measurements, the single-minute limits of detection are derived based on the 3σ variation in the recorded HEPA background signals. Hence, 3σ limits of detection were found to be between 19 and 46 pg m^{-3} for all detected PAH signals reported herein.

The instrumental stability and separation capability, sufficient time resolution, good response to temporal variations, and low limits of detection, not only for the PAHs but also for a wide range other organics, result in a good data quality that provides a good basis for source apportionment.

3.2 Source apportionment

To obtain a both quantitative and qualitative reconstruction of the time series based on mass spectral information assigned to different factors, we performed a NMF with NNDSVD initialization. Subsequently, the sources or physicochemical processes are identified from the chemical information in the factor mass spectra (e.g., via well-known tracer compounds) and/or by looking at the temporal or diurnal variations (e.g., to understand local emissions of the industrial area).

During the automated analysis of the dataset, the number of factors, representing the sources and processes, was subsequently increased. Using 10 separate factors for the NMF leads to a sufficient reduction in the cost function, whereas the inclusion of more factors did not further improve the accuracy of the reconstruction and, hence, did not add more chemical information.

The time series of these 10 identified factors are displayed in Fig. 3a. Note that the sum of the 10 factors equals the trace of total organics (with only a negligible residual; see Fig. S3 for more detail). Figure 3b, c and d show the reconstructed mass spectra for a mixed aged oxygenated organic aerosol (OOA), fresh biomass burning organic aerosol (BBOA) and cigarette smoke organic aerosol (CSOA), respectively.

These three factors are selected as they include the majority of PAH-related information. The mass spectra (Fig. S4) and diurnal variations (Fig. S5) of all 10 identified factors are presented in the Supplement. Detailed description and inter-

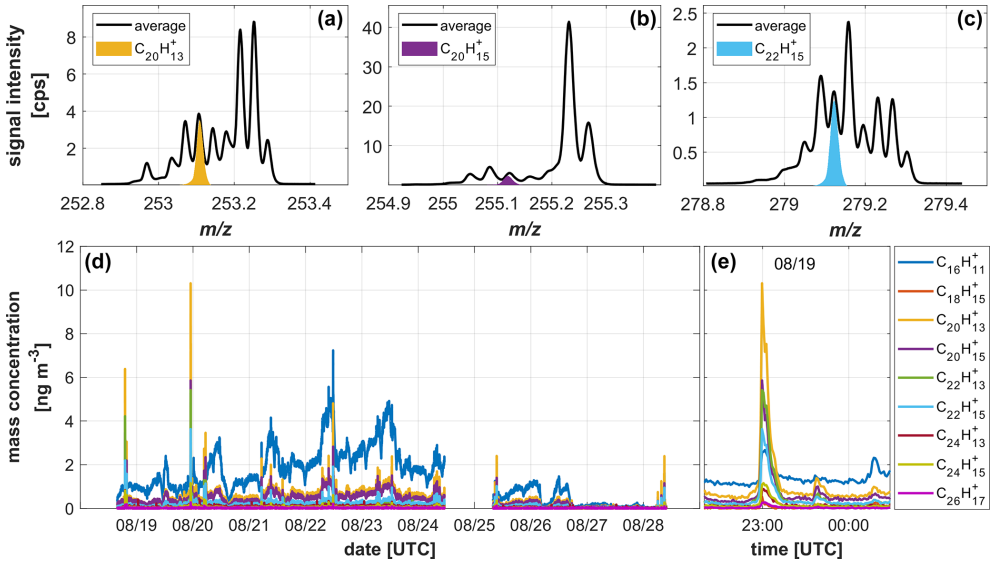

Figure 2. Three exemplary peak systems of the PAH signals $C_{20}H_{13}^+$, $C_{20}H_{15}^+$ and $C_{22}H_{15}^+$ (campaign average, **a–c**). Panel **(d)** shows time traces of all nine ionic signals from PAHs detected in the particle phase, while panel **(e)** presents a close-up view of the evening hours of 19 August 2024.

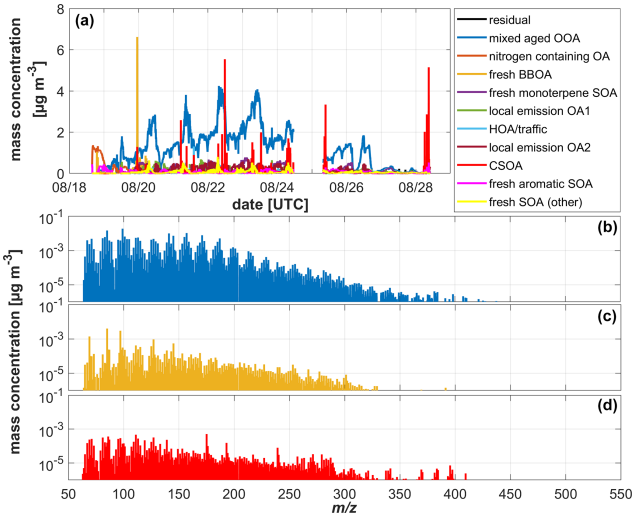

Figure 3. Time traces of the 10 identified factors are shown in panel **(a)**. Panels **(b)**, **(c)** and **(d)** depict the reconstructed mass spectra for a mixed aged oxygenated organic aerosol (OOA; blue), fresh biomass burning organic aerosol (BBOA; orange) and cigarette smoke organic aerosol (CSOA; red), respectively.

pretation of all factors, including their associated sources and processes, lie outside the scope of this study.

The most dominant factor contains a plethora of compounds but is predominantly composed of mixed aged OOA with compounds like levoglucosan and pinonic acid in different oxidation states. This factor generally shows the highest mass concentrations before noon, drops slightly in the afternoon but stays dominant during night. Our understanding is that this factor mostly contributes to the accumulation of condensed organics during the stable weather period. Hence, this complex factor could not be separated any further while introducing more NMF factors.

Another factor that shows two distinct spikes on the first weekend is attributed to fresh biomass burning. As can be seen in the mass spectrum in Fig. 3c, the factor contains the mass spectral signature of the anhydro-sugar levoglucosan (m/z 85.028, 127.039, 145.050 and 163.060), a well-known particulate tracer for biomass burning. Because these are singular events on the first weekend with sunny and dry weather, the source could potentially be a nearby camp fire or barbecue.

During working hours, another prominent source of organic aerosol is cigarette smoke, most likely from smokers around the building and on the building's balconies. Even in 2024, cigarette smoking is a widespread habit in Austria (Dorner et al., 2020). The mass spectrum of the respective factor (Fig. 3d) shows the expected compounds found in cigarette smoke, like nicotine and scopoletin (e.g., Arndt et al., 2020).

Following the separation of the total condensed organics into different factors and the subsequent assignment of distinct sources to each factor, we investigate how these sources contribute to the emission of condensed PAHs.

Figure 4 shows the time series of two exemplary PAH signals (panel a: $C_{20}H_{13}^+$; panel b: $C_{22}H_{13}^+$) that are selected to represent two separate emission groups. Colored traces show the individual NMF factors that contribute to the recorded signals. Three factors, i.e., mixed aged OOA, fresh BBOA and CSOA, show the highest contribution to $C_{20}H_{13}^+$. On the other hand, $C_{22}H_{13}^+$ is dominated by the fresh BBOA emis-

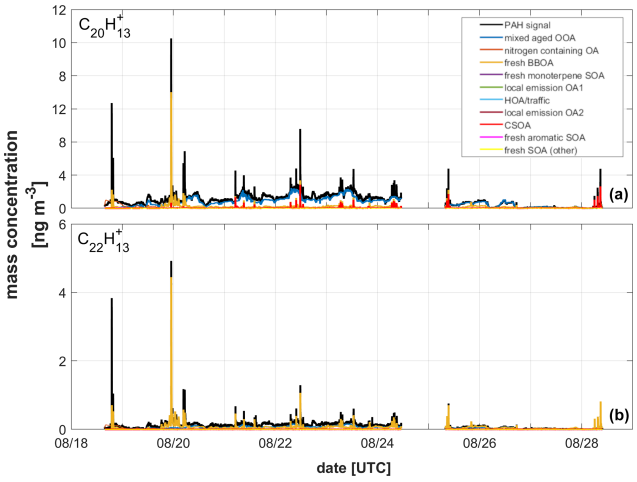

Figure 4. Time series of two selected PAH signals (black), $C_{20}H_{13}+$ **(a)** and $C_{22}H_{13}+$ **(b)**, that are selected to represent two separate emission groups. Colored traces show the individual NMF factors that contribute to the recorded signals.

sion factor. Obviously, fresh BBOA and CSOA coincide during times of cigarette smoke plumes, but NMF still is capable of separating the biomass burning fraction from a cigarette-specific factor within these short plumes, highlighting the general separation capability of this factorization method.

Also important to note is that traffic emissions only play a subordinate role in the processes associated with PAH emissions during the time of our observations.

4 Conclusions

We have successfully coupled a redesigned FUSION PTR-TOF 10k to a CHARON particle inlet with an improved aerodynamic lens system for particle enrichment. With this instrument, organic aerosol in Innsbruck, Austria, was analyzed over the course of 11 d in August 2023. The high sensitivity of the FUSION RF ion–molecule reactor ($S =$ 15 000–20 000 cps ppb V^{-1} at an extended mass range up to m/z 719) combined with the enrichment factor of 20 for particles in the size range from 100 nm to > 1 µm allowed the measurement of mass concentrations in the low double-digit picogram-per-cubic-meter range with 1 min time resolution. Furthermore, the identification capability of the high-mass-resolution TOF-MS ($R > 14\,000$) enabled the separation of the complex mass spectra into more than 4000 ionic signals of organic aerosol. Among those thousands of signals, we were able to identify a series of nine chemical compositions that represent a series of PAHs. Mass concentrations of these PAHs from 0 to 11 ng m^{-3} are recorded; single-minute 3σ limits of detection were found to be between 19 and 46 pg m^{-3}.

Factorization of the entire dataset showed 10 separate sources and processes that affect the organic aerosol concentration and composition. Out of these 10 identified factors, 3 show significant contributions of PAHs: a mixed aged OOA factor, fresh BBOA and CSOA, contributing to 63 %, 19 % and 6 % of the total PAH signal, respectively. No significant contribution of PAHs could be identified in the traffic-related factor (0.4 %).

All presented results and methods act as a proof-of-principle study that demonstrates the unprecedented analytical performance of the CHARON FUSION PTR-TOF 10k. However, due to the complexity of the recorded data, interpretation of the vast majority of signals and associated factors exceeds the scope of this paper. Hence, interesting trends, including repetitive short-term spikes, diurnal variations and the impact of changing weather conditions, affecting the chemical composition of organic aerosol, could not be studied in detail.

Future work will include an exploration of other, even softer, ionization techniques, like soft ammonium adduct ionization (A.NH4+), which has been reported to conserve the chemical composition of a plethora of oxygenated organic compounds (e.g., Müller et al., 2020; Reinecke et al., 2023). This conservation of chemical information and a high selectivity to oxygenated organic compounds will allow for even deeper insights into primary emission and secondary formation processes of particulate oxygenated organic species in the atmosphere.

Data availability. All data can be provided upon request by the corresponding author.

Supplement. The supplement related to this article is available online at: https://doi.org/10.5194/ar-2-225-2024-supplement.

Author contributions. MM and TR conducted all hardware modifications to enable the coupling of the FUSION and CHARON. AK designed the improved aerodynamic lens system and supported implementing the experimental setup. MM, ML and TR conducted the measurements, analyzed the data and wrote the manuscript.

Competing interests. Tobias Reinecke, Markus Leiminger, Andreas Klinger and Markus Müller work for IONICON Analytik GmbH, which is commercializing CHARON and the FUSION PTR-TOF 10k.

Disclaimer. Publisher's note: Copernicus Publications remains neutral with regard to jurisdictional claims made in the text, published maps, institutional affiliations, or any other geographical representation in this paper. While Copernicus Publications makes ev-

ery effort to include appropriate place names, the final responsibility lies with the authors.

Financial support. Parts of this research have been supported by the Austrian Research Promotion Agency (FFG) within the framework of the pSAT project (grant no. FO999900547).

Review statement. This paper was edited by Hilkka Timonen and reviewed by Johannes Passig and one anonymous referee.

References

Agudelo-Castañeda, D. M., Teixeira, E. C., Schneider, I. L., Lara, S. R., and Silva, L. F. O.: Exposure to polycyclic aromatic hydrocarbons in atmospheric $PM_{1.0}$ of urban environments: Carcinogenic and mutagenic respiratory health risk by age groups, Environ. Pollut., 224, 158–170, https://doi.org/10.1016/j.envpol.2017.01.075, 2017.

Arndt, D., Wachsmuth, C., Buchholz, C., and Bentley, M.: A complex matrix characterization approach, applied to cigarette smoke, that integrates multiple analytical methods and compound identification strategies for non-targeted liquid chromatography with high-resolution mass spectrometry, Rapid Commun. Mass Spectrom., 34, e8571, https://doi.org/10.1002/rcm.8571, 2020.

Borrás, E. and Tortajada-Genaro, L. A.: Characterisation of polycyclic aromatic hydrocarbons in atmospheric aerosols by gas chromatography-mass spectrometry, Anal. Chim. Acta, 583, 266–276, https://doi.org/10.1016/j.aca.2006.10.043, 2007.

Bosque, R. and Sales, J.: Polarizabilities of Solvents from the Chemical Composition, J. Chem. Inf. Comput. Sci., 42, 1154–1163, https://doi.org/10.1021/ci025528x, 2002.

Boutsidis, C. and Gallopoulos, E.: SVD based initialization: A head start for nonnegative matrix factorization, Pattern Recognition, 41, 1350–1362, https://doi.org/10.1016/j.patcog.2007.09.010, 2008.

Choi, H., Harrison, R., Komulainen, H., and Saborit, J. M. D.: Polycyclic aromatic hydrocarbons, in: WHO Guidelines for Indoor Air Quality: Selected Pollutants, World Health Organization, 289–346 pp., 2010.

Dorner, T. E., Brath, H., and Kautzky-Willer, A.: Sex-specific trends in smoking prevalence over seven years in different Austrian populations: results of a time-series cross-sectional analysis, BMJ Open, 10, e035235, https://doi.org/10.1136/bmjopen-2019-035235, 2020.

Dzepina, K., Arey, J., Marr, L. C., Worsnop, D. R., Salcedo, D., Zhang, Q., Onasch, T. B., Molina, L. T., Molina, M. J., and Jimenez, J. L.: Detection of particle-phase polycyclic aromatic hydrocarbons in Mexico City using an aerosol mass spectrometer, Int. J. Mass Spectro., 263, 152–170, https://doi.org/10.1016/j.ijms.2007.01.010, 2007.

Eichler, P., Müller, M., D'Anna, B., and Wisthaler, A.: A novel inlet system for online chemical analysis of semi-volatile submicron particulate matter, Atmos. Meas. Tech., 8, 1353–1360, https://doi.org/10.5194/amt-8-1353-2015, 2015.

Eriksson, A. C., Nordin, E. Z., Nyström, R., Pettersson, E., Swietlicki, E., Bergvall, C., Westerholm, R., Boman, C., and Pagels, J. H.: Particulate PAH Emissions from Residential Biomass Combustion: Time-Resolved Analysis with Aerosol Mass Spectrometry, Environ. Sci. Technol., 48, 7143–7150, https://doi.org/10.1021/es500486j, 2014.

Graus, M., Müller, M., and Hansel, A.: High resolution PTR-TOF: Quantification and formula confirmation of VOC in real time, J. Am. Soc. Mass Spectrom., 21, 1037–1044, https://doi.org/10.1016/j.jasms.2010.02.006, 2010.

Gueneron, M., Erickson, M. H., VanderSchelden, G. S., and Jobson, B. T.: PTR-MS fragmentation patterns of gasoline hydrocarbons, Int. J. Mass Spectro., 379, 97–109, https://doi.org/10.1016/j.ijms.2015.01.001, 2015.

Hansel, A., Jordan, A., Holzinger, R., Prazeller, P., Vogel, W., and Lindinger, W.: Proton transfer reaction mass spectrometry: online trace gas analysis at the ppb level, Int. J. Mass Spectro. Ion Process., 149–150, 609–619, https://doi.org/10.1016/0168-1176(95)04294-U, 1995.

Herring, C. L., Faiola, C. L., Massoli, P., Sueper, D., Erickson, M. H., McDonald, J. D., Simpson, C. D., Yost, M. G., Jobson, B. T., and VanReken, T. M.: New Methodology for Quantifying Polycyclic Aromatic Hydrocarbons (PAHs) Using High-Resolution Aerosol Mass Spectrometry, Aerosol Sci. Technol., 49, 1131–1148, https://doi.org/10.1080/02786826.2015.1101050, 2015.

Karl, T., Gohm, A., Rotach, M. W., Ward, H. C., Graus, M., Cede, A., Wohlfahrt, G., Hammerle, A., Haid, M., Tiefengraber, M., Lamprecht, C., Vergeiner, J., Kreuter, A., Wagner, J., and Staudinger, M.: Studying Urban Climate and Air Quality in the Alps: The Innsbruck Atmospheric Observatory, B. Am. Meteorol. Soc., 101, E488–E507, https://doi.org/10.1175/BAMS-D-19-0270.1, 2020.

Kaur, S., Senthilkumar, K., Verma, V. K., Kumar, B., Kumar, S., Katnoria, J. K., and Sharma, C. S.: Preliminary Analysis of Polycyclic Aromatic Hydrocarbons in Air Particles (PM_{10}) in Amritsar, India: Sources, Apportionment, and Possible Risk Implications to Humans, Arch. Environ. Contam. Toxicol., 65, 382–395, https://doi.org/10.1007/s00244-013-9912-6, 2013.

Laskin, J., Laskin, A., and Nizkorodov, S. A.: Mass Spectrometry Analysis in Atmospheric Chemistry, Anal. Chem., 90, 166–189, https://doi.org/10.1021/acs.analchem.7b04249, 2018.

Leglise, J., Müller, M., Piel, F., Otto, T., and Wisthaler, A.: Bulk Organic Aerosol Analysis by Proton-Transfer-Reaction Mass Spectrometry: An Improved Methodology for the Determination of Total Organic Mass, O:C and H:C Elemental Ratios, and the Average Molecular Formula, Anal. Chem., 91, 12619–12624, https://doi.org/10.1021/acs.analchem.9b02949, 2019.

Lung, S.-C. C. and Liu, C.-H.: Fast analysis of 29 polycyclic aromatic hydrocarbons (PAHs) and nitro-PAHs with ultra-high performance liquid chromatography-atmospheric pressure photoionization-tandem mass spectrometry, Sci. Rep., 5, 12992, https://doi.org/10.1038/srep12992, 2015.

Müller, M., Mikoviny, T., Jud, W., D'Anna, B., and Wisthaler, A.: A new software tool for the analysis of high resolution PTR-TOF mass spectra, Chemometr. Intell. Lab., 127, 158–165, https://doi.org/10.1016/j.chemolab.2013.06.011, 2013.

Müller, M., Eichler, P., D'Anna, B., Tan, W., and Wisthaler, A.: Direct Sampling and Analysis of Atmospheric Particulate Organic Matter by Proton-Transfer-Reaction

Mass Spectrometry, Anal. Chem., 89, 10889–10897, https://doi.org/10.1021/acs.analchem.7b02582, 2017.

Müller, M., Piel, F., Gutmann, R., Sulzer, P., Hartungen, E., and Wisthaler, A.: A novel method for producing NH_4^+ reagent ions in the hollow cathode glow discharge ion source of PTR-MS instruments, Int. J. Mass Spectro., 447, 116254, https://doi.org/10.1016/j.ijms.2019.116254, 2020.

Passig, J., Schade, J., Irsig, R., Kröger-Badge, T., Czech, H., Adam, T., Fallgren, H., Moldanova, J., Sklorz, M., Streibel, T., and Zimmermann, R.: Single-particle characterization of polycyclic aromatic hydrocarbons in background air in northern Europe, Atmos. Chem. Phys., 22, 1495–1514, https://doi.org/10.5194/acp-22-1495-2022, 2022.

Patel, A. B., Shaikh, S., Jain, K. R., Desai, C., and Madamwar, D.: Polycyclic Aromatic Hydrocarbons: Sources, Toxicity, and Remediation Approaches, Front. Microbiol., 11, 562813, https://doi.org/10.3389/fmicb.2020.562813, 2020.

Piel, F., Müller, M., Mikoviny, T., Pusede, S. E., and Wisthaler, A.: Airborne measurements of particulate organic matter by proton-transfer-reaction mass spectrometry (PTR-MS): a pilot study, Atmos. Meas. Tech., 12, 5947–5958, https://doi.org/10.5194/amt-12-5947-2019, 2019.

Piel, F., Müller, M., Winkler, K., Skytte af Sätra, J., and Wisthaler, A.: Introducing the extended volatility range proton-transfer-reaction mass spectrometer (EVR PTR-MS), Atmos. Meas. Tech., 14, 1355–1363, https://doi.org/10.5194/amt-14-1355-2021, 2021.

Poulain, L., Iinuma, Y., Müller, K., Birmili, W., Weinhold, K., Brüggemann, E., Gnauk, T., Hausmann, A., Löschau, G., Wiedensohler, A., and Herrmann, H.: Diurnal variations of ambient particulate wood burning emissions and their contribution to the concentration of Polycyclic Aromatic Hydrocarbons (PAHs) in Seiffen, Germany, Atmos. Chem. Phys., 11, 12697–12713, https://doi.org/10.5194/acp-11-12697-2011, 2011.

Reinecke, T., Leiminger, M., Jordan, A., Wisthaler, A., and Müller, M.: Ultrahigh Sensitivity PTR-MS Instrument with a Well-Defined Ion Chemistry, Anal. Chem., 95, 11879–11884, https://doi.org/10.1021/acs.analchem.3c02669, 2023.

Schade, J., Passig, J., Irsig, R., Ehlert, S., Sklorz, M., Adam, T., Li, C., Rudich, Y., and Zimmermann, R.: Spatially Shaped Laser Pulses for the Simultaneous Detection of Polycyclic Aromatic Hydrocarbons as well as Positive and Negative Inorganic Ions in Single Particle Mass Spectrometry, Anal. Chem., 91, 10282–10288, https://doi.org/10.1021/acs.analchem.9b02477, 2019.

Sekimoto, K., Li, S.-M., Yuan, B., Koss, A., Coggon, M., Warneke, C., and de Gouw, J.: Calculation of the sensitivity of proton-transfer-reaction mass spectrometry (PTR-MS) for organic trace gases using molecular properties, Int. J. Mass Spectro., 421, 71–94, https://doi.org/10.1016/j.ijms.2017.04.006, 2017.

Su, T. and Chesnavich, W. J.: Parametrization of the ion–polar molecule collision rate constant by trajectory calculations, The J. Chem. Phys., 76, 5183–5185, https://doi.org/10.1063/1.442828, 1982.

Thrane, K. E. and Mikalsen, A.: High-volume sampling of airborne polycyclic aromatic hydrocarbons using glass fibre filters and polyurethane foam, Atmos. Environ. (1967), 15, 909–918, https://doi.org/10.1016/0004-6981(81)90090-1, 1981.

Ulbrich, I. M., Canagaratna, M. R., Zhang, Q., Worsnop, D. R., and Jimenez, J. L.: Interpretation of organic components from Positive Matrix Factorization of aerosol mass spectrometric data, Atmos. Chem. Phys., 9, 2891–2918, https://doi.org/10.5194/acp-9-2891-2009, 2009.

Wisthaler, A., Müller, M., Poulain, L., Piel, F., Gräfe, R., Spindler, G., Wiedensohler, A., and Herrmann, H.: Chemical Characterization of Particulate and Volatile Organic Compounds in the Rural Wintertime Atmosphere by CHARON PTR-ToF-MS, EGU General Assembly 2020, Online, 4–8 May 2020, EGU2020-19635, https://doi.org/10.5194/egusphere-egu2020-19635, 2020.

Xu, P., Yang, Y., Zhang, J., Gao, W., Liu, Z., Hu, B., and Wang, Y.: Characterization and source identification of submicron aerosol during serious haze pollution periods in Beijing, J. Environ. Sci., 112, 25–37, https://doi.org/10.1016/j.jes.2021.04.005, 2022.

Yassine, M. M., Harir, M., Dabek-Zlotorzynska, E., and Schmitt-Kopplin, P.: Structural characterization of organic aerosol using Fourier transform ion cyclotron resonance mass spectrometry: Aromaticity equivalent approach, Rapid Commun. Mass Spectro., 28, 2445–2454, https://doi.org/10.1002/rcm.7038, 2014.

Yuan, B., Koss, A. R., Warneke, C., Coggon, M., Sekimoto, K., and de Gouw, J. A.: Proton-Transfer-Reaction Mass Spectrometry: Applications in Atmospheric Sciences, Chem. Rev., 117, 13187–13229, https://doi.org/10.1021/acs.chemrev.7b00325, 2017.